Batteries & Supercaps

Research Article
doi.org/10.1002/batt.202400578

Chemistry Europe
European Chemical Societies Publishing

www.batteries-supercaps.org

Precipitating Zinc-Polyethylenimine Complex for Long-Lasting Aqueous Zn-I Batteries

Kaiqiang Zhang,*[a] Chao Wu,[a] Luoya Wang,[a] Changlong Ma,[a] Pei Kong,[a] Kun Zhuang,[a] Jilei Ye,*[a] and Yuping Wu[a]

Aqueous rechargeable Zn–I battery offers significant advantages for reliable and cost-effective energy storage applications. However, current aqueous Zn–I batteries still face challenges related to limited cycling performance. Herein, we introduce an innovative in-situ precipitated zinc-polyethylenimine (PEI-Zn^{2+}) complex design. This approach leverages the complexing effect between Zn^{2+} cations from the aqueous electrolyte and the amino groups of PEI in the cathode, enhancing the performance of aqueous Zn–I batteries. The resulting insoluble PEI-Zn^{2+} complex immobilizes iodide species, facilitating efficient battery operation. This novel design enabled an aqueous Zn–I battery to achieve over 5000 cycles with 83.3% capacity retention. Additionally, the battery demonstrated promising preliminary performance under practical conditions, including fluctuating charging, various states of charge, and integration with photovoltaic solar panels. This work provides new insights into the design of aqueous zinc batteries.

Introduction

Aqueous rechargeable Zn–I batteries are a promising and reliable energy storage solution for static energy storage applications, such as integration with solar and wind power systems.[1,2] However, current aqueous Zn–I secondary batteries still face challenges, including limited cycling capability and a complicated manufacturing process.[3,4] Enhancing long-term cycling capability and simplifying battery production can help reduce deployment and maintenance costs, making these batteries more suitable for practical large-scale energy storage applications.[5,6]

Significant progress has been made in improving aqueous Zn–I batteries.[7,8] Various cathodic adsorption and fixation materials for iodide species have been developed, showing substantial performance enhancements.[9,10] In addition to advancements in cathode materials, membrane modifications have also proven effective in enhancing aqueous Zn–I battery performance.[11,12] However, further innovations that are both facile and effective are still required to push the boundaries of current research on aqueous Zn–I batteries.

The amino functional group is well-known for its ability to complex with metal cations, such as Zn^{2+}, Cu^{2+}, and Co^{2+}, for metal ions adsorption applications due to its lone pair of electrons of amino group, which offers a potential strategy for designing polymer-based electrode materials for aqueous Zn–I batteries.[13–15] The Zn–I battery's aqueous electrolyte contains abundant Zn^{2+} cations that can be utilized to form an in-situ complex with amino functional groups, resulting in a stable, insoluble complex within the cathode. Polyethylenimine (PEI) is a water-soluble polymeric material rich in amino functional groups, ideal for creating such a complex network. Therefore, we propose an in-situ precipitated PEI-Zn^{2+} complex electrode design, leveraging the complexing interaction between Zn^{2+} cations from the aqueous electrolyte and the amino functional groups of PEI in cathode (Figure 1a) to enhance current aqueous Zn–I battery performance. The formation of PEI-Zn^{2+} complex is irreversible and the formed product is insoluble in the aqueous electrolyte (Figure 1b). The pre-introduced iodide species can be rationally immobilized within this PEI-Zn^{2+} complex in cathode, enabling the fundamental construction of Zn–I battery.

Based on this battery design concept, the constructed aqueous rechargeable Zn–I battery demonstrates stable cycling performance of over 5000 cycles and maintains compatibility with various operating conditions, including fluctuating charge current densities, different states of charge, and fast-charging. Additionally, it integrates effectively with photovoltaic solar panel charging under natural sunlight. This innovative battery design offers a versatile platform for advancing long-lasting, high-performance aqueous zinc batteries.

Demonstration of PEI-Zn^{2+} Complexing Effect

The complexing effect between Zn^{2+} cations and PEI was visually demonstrated through a series of experiments. Specifically, an aqueous solution containing PEI and ZnI_2 (see Methods for more details) was introduced into a 2 M $ZnSO_4$ aqueous solution, which functions as the electrolyte in the following battery assembly. Initially, the PEI-containing solution and the $ZnSO_4/H_2O$ solution remained immiscible, forming distinct liquid layers (Figure 1b, top-left). Upon manual mixing, white sediment formed in the solution, suggesting the generation of

[a] K. Zhang, C. Wu, L. Wang, C. Ma, P. Kong, K. Zhuang, J. Ye, Y. Wu
School of Energy Sciences and Engineering, Nanjing Tech University, Nanjing, Jiangsu Province 211816, China
E-mail: kaiqiangzhang@njtech.edu.cn
yejilei@njtech.edu.cn

Supporting information for this article is available on the WWW under https://doi.org/10.1002/batt.202400578

Research Article
doi.org/10.1002/batt.202400578
Chemistry Europe
European Chemical Societies Publishing

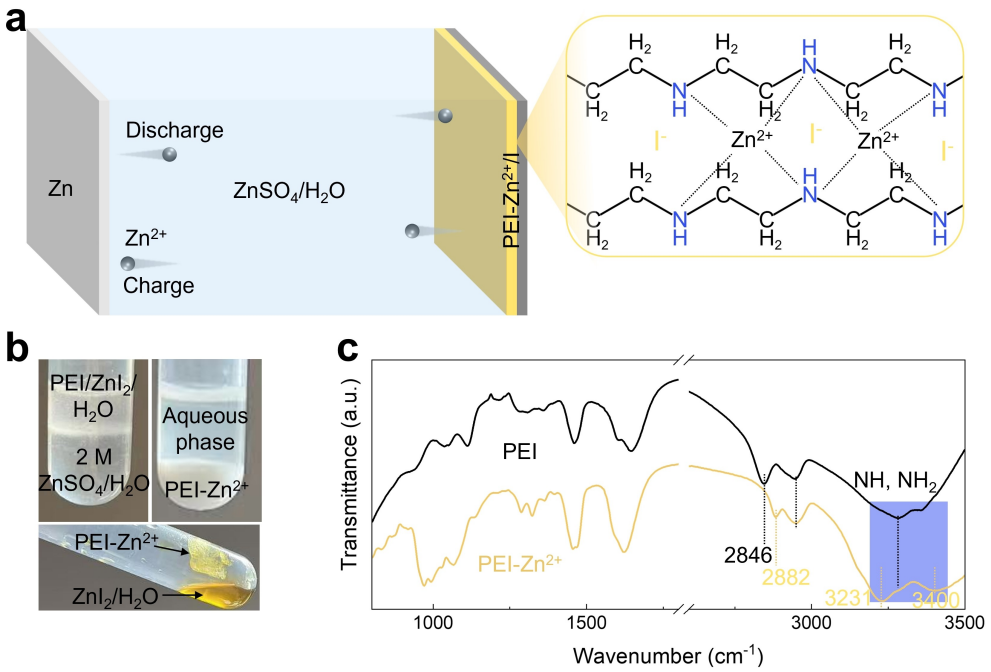

Figure 1. (a) Schematic illustration of the aqueous Zn–I battery with the iodide species fixed by PEI-Zn^{2+} complex. (b) Adding the PEI/ZnI_2/H_2O solution in 2 M $ZnSO_4$/H_2O solution before (top-left) and after (top-right) manual shaking and in 5 M ZnI_2/H_2O solution (bottom). (c) FTIR spectra of PEI and PEI-Zn^{2+} complex.

an insoluble PEI-Zn^{2+} complex (Figure 1b and Video S1). However, one concern may be the absence of this PEI-Zn^{2+} complex in the original PEI/ZnI_2/H_2O solution. This can be attributed to the limited amount of Zn^{2+} cations, resulting in only a small quantity of PEI-Zn^{2+} complex that remains below the saturation limit. To test this, we increased the Zn^{2+} cation concentration by adding the same PEI/ZnI_2/H_2O solution to a 5 M ZnI_2/H_2O solution. As expected, this led to consistent formation of the insoluble PEI-Zn^{2+} complex (Figure 1b, bottom). The yellow color of ZnI_2 solution arises from oxidization of iodide species by ambient environment.

The PEI-Zn^{2+} complex was analyzed using Fourier transform infrared (FTIR) spectroscopy. After complexation with Zn^{2+}, significant shifts in the –NH and –NH_2 bond vibrations in PEI were observed, including a new peak at 3231 cm^{-1} and a significant shift from 2846 cm^{-1} to 2882 cm^{-1} (Figure 1c).[16] These changes indicate that the presence of positively charged Zn^{2+} cations influences the original bond vibrations of PEI, particularly in the amino functional groups. Furthermore, the PEI-Zn^{2+} complex is insoluble in H_2O, as attempts to redisperse the white PEI-Zn^{2+} complex in H_2O resulted in a uniform suspension (Figure S1a and Video S2, Supporting Information). This confirms that the formation of PEI-Zn^{2+} complex is irreversible, effectively preventing the undesired mixing of cathode and supporting prolonged battery cycling performance. Additionally, the FTIR spectrum of the aqueous phase in the $ZnSO_4$/H_2O/PEI-Zn^{2+} mixture shows no distinct PEI signal (Figure S1b, Supporting Information), verifying sufficient amount of Zn^{2+} cations for complete complexation with the PEI in cathode.

This property is advantageous for battery construction, as it allows the redox-active species to be securely immobilized within the PEI-Zn^{2+} complex. The complexing effect between PEI and various metal cations was further demonstrated using 1 M $ZnCl_2$/H_2O, 0.7 M $Al_2(SO_4)_3$/H_2O, 1 M $CuSO_4$/H_2O, and 1 M Li_2SO_4/H_2O solutions. $ZnCl_2$/H_2O and $Al_2(SO_4)_3$/H_2O showed a consistent phase separation phenomenon (Figure S1c,d and Videos S3 and S4, Supporting Information). When using $CuSO_4$/H_2O, the typical transparent blue aqueous solution turned dark immediately (Figure S1e,f and Video S5, Supporting Information). However, the Li_2SO_4/H_2O solution showed no significant change, remaining transparent (Figure S1g and Video S6, Supporting Information).

Electrochemical Performance

The electrochemical performance of the aqueous Zn–I battery was evaluated using cyclic voltammetry (CV) scanning from 0.8 to 1.6 V vs. Zn/Zn^{2+} at a scan rate of 4 mV s^{-1}. The CV curve exhibited a pair of redox peaks characteristics of the iodide redox process (Figure 2a), confirming the successful operation of the designed aqueous Zn–I battery. The rate performance of the battery was further analyzed through galvanostatic charging and discharging at current densities of 0.05, 0.1, 0.2, 0.3, 0.4, and 0.5 mA cm^{-2}. The battery demonstrated an 88.9% discharge capacity retention, decreasing from 199.4 to 177.2 mAh g^{-1} as the current density increased from 0.05 to 0.5 mA cm^{-2}, while maintaining a consistent redox plateau for each current density (Figure 2b,c). These results preliminarily validate the efficacy of our aqueous Zn–I battery design leveraging the PEI-Zn^{2+} complexing effect. The battery also exhibited an electrochemical impedance of approximately 60 Ohms (Figure S2a, Supporting Information), suggesting appropriate electrochemical impe-

Research Article
doi.org/10.1002/batt.202400578
Chemistry Europe
European Chemical Societies Publishing

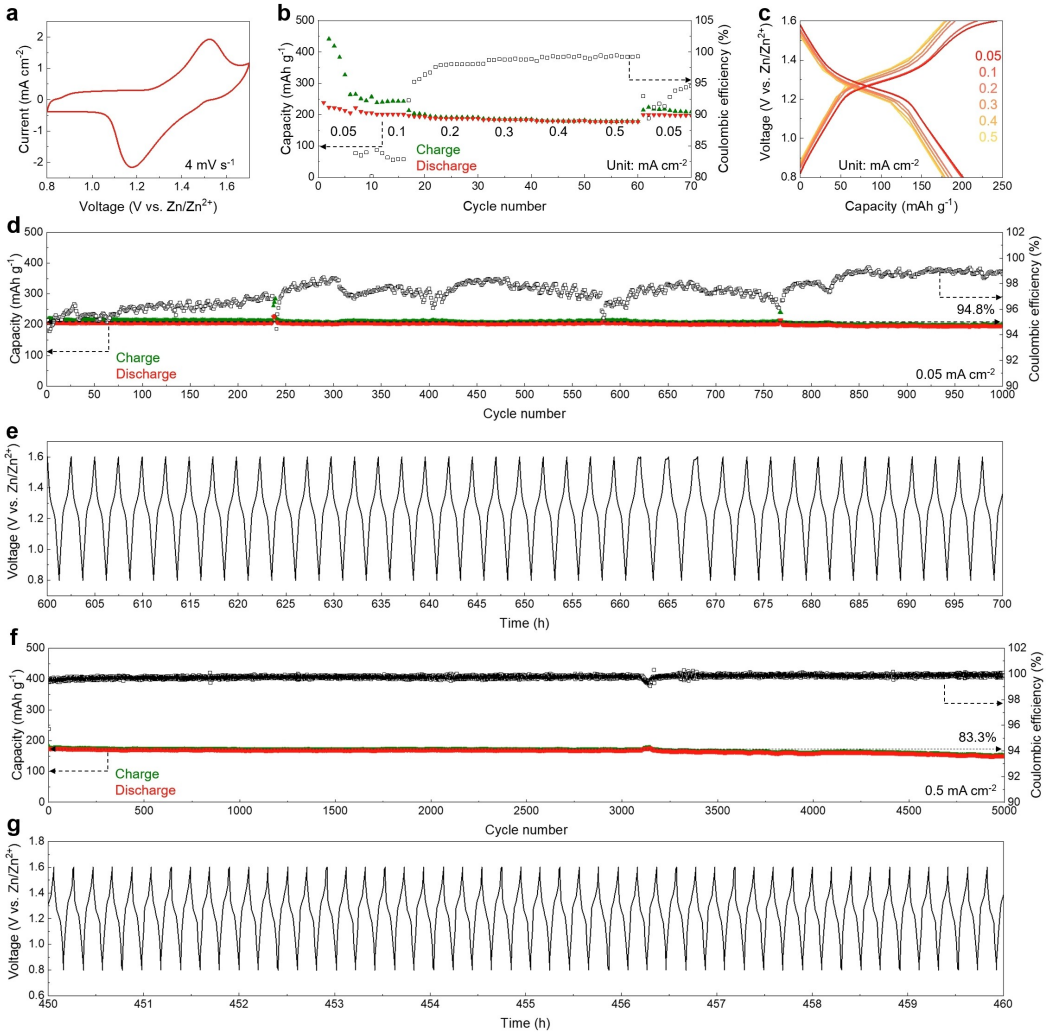

Figure 2. Electrochemical performance of the aqueous Zn–I battery. (a-c) CV curve scanned at 4 mV s^{-1} (a), rate performance (b) and corresponding voltage profiles (c) of the battery. (d–g) Cycling tests and corresponding voltage profiles at 0.05 (d,e) and 0.5 mA cm^{-2} (f,g).

dance. Further electrochemical kinetics analysis was conducted using redox peak polarization scanned at 4, 6, 8, and 10 mV s^{-1}, revealing a 0.07 V redox hysteresis (Figure S2b, Supporting Information). The relationship between peak and capacitive currents vs. scanning rates has been analyzed. The voltage increases from 0.8 to 1.7 V vs. Zn/Zn^{2+} shows an inverse relationship with the scan rate (Figure S2c). Assuming a constant amount of redox-active species is consumed during each period, the peak current gradually decreases as the scanning rate increases (Figure S2d), while the capacitive current displays a linear increase (Figure S2e,f). These results indicate that the battery exhibits sufficient charge carrier migration kinetics, as evidenced by the capacitive current in the redox-inactive region and demonstrates decent redox kinetics.

Long-term performance tests were conducted to reinforce the battery design concept. The battery underwent repeated charging and discharging at 0.05 and 0.5 mA cm^{-2}. It exhibited a specific capacity retention of 94.8% after 1000 cycles (Figure 2d). The voltage variation profiles during cycling tests confirmed the battery's consistent performance (Figure 2e). At a higher current density of 0.5 mA cm^{-2}, the battery demonstrated stable performance over 5000 cycles, retaining 83.3% of its initial capacity retention (Figure 2f). Consistent voltage variation profiles were observed (Figure 2g). The long-term cycling capability of the battery was further confirmed at 0.5 mA cm^{-2}, with an 83.5% capacity retention over 3000 cycles (Figure S3a, Supporting Information). During operation, the battery displayed consistent voltage profiles (Figure S3b, Supporting Information). These results, when compared to other studies, highlight the long-term cycling stability of the aqueous Zn–I battery, which utilizes the PEI-Zn^{2+} complex for effectively confining redox-active iodide species (Table S1).

Research Article
doi.org/10.1002/batt.202400578
Chemistry Europe
European Chemical Societies Publishing

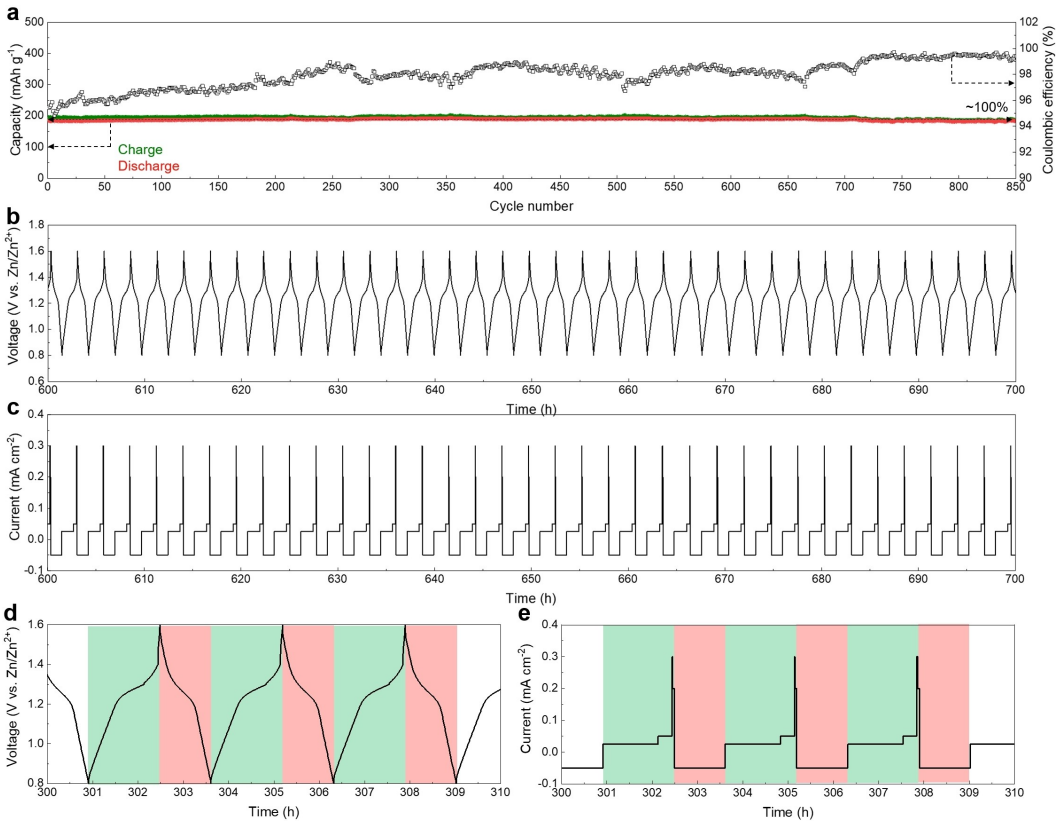

Figure 3. Fluctuating charge tests of the aqueous Zn–I battery. (a) Battery capacity during the tests. (b,d) Representative voltage and (c,e) current profiles tracked during battery tests.

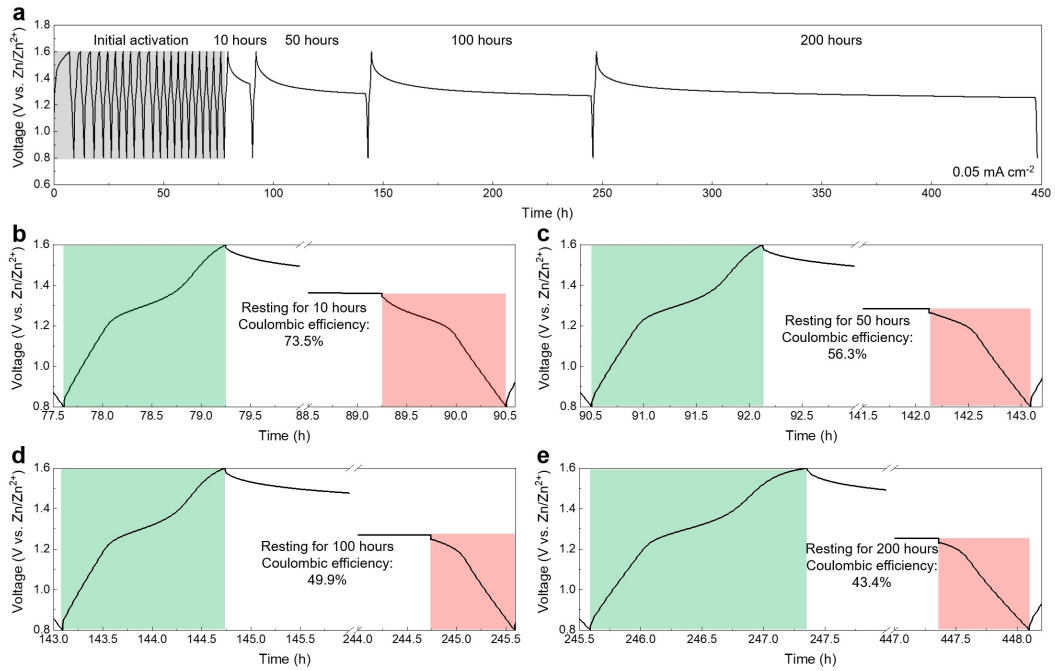

Figure 4. Self-discharging tests of the aqueous Zn–I battery. (a–e) Overall voltage profiles (a) and voltage profiles when resting for 10 (b), 50 (c), 100 (d), and 200 hours (e).

Research Article
doi.org/10.1002/batt.202400578
Chemistry Europe
European Chemical Societies Publishing

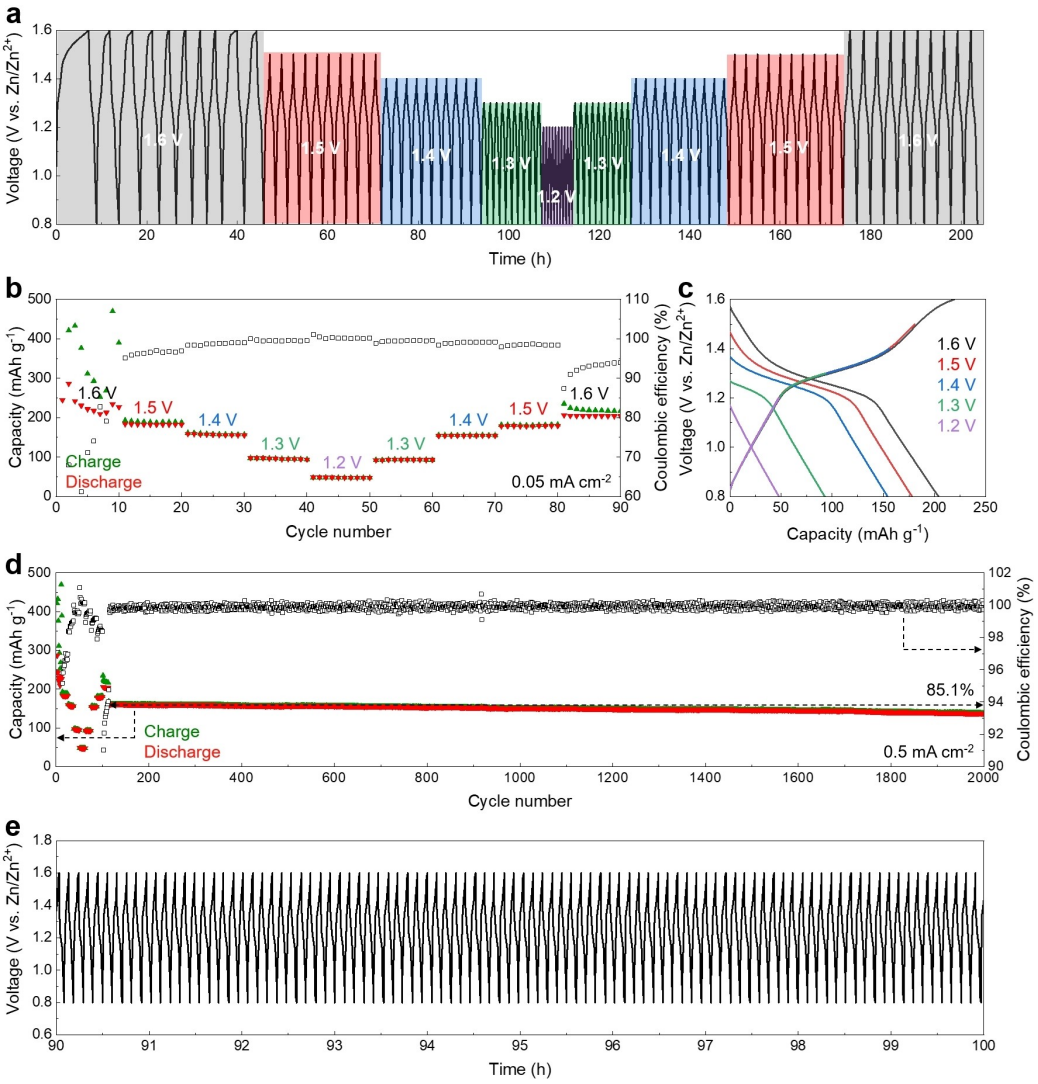

Figure 5. Compatibility of the aqueous Zn–I battery with various charging states. (a) Continuous voltage profiles, (b) specific capacities, and (c) representative voltage profiles during the tests. (d) Specific capacities and Coulombic efficiencies of repeated cycling tests after the charging status compatibility tests. (e) Voltage profiles tracked during the test.

Electrochemical Performance under Various Conditions

Fluctuating Charge

Integrating batteries with practical photovoltaic solar panels or wind powers, often involves dealing with naturally fluctuating power supplies.[17,18] To demonstrate the potential compatibility of the aqueous Zn–I battery with such natural green energy sources, we tested its performance under fluctuating charge current densities to simulate these conditions. Specifically, the battery was charged to 1.6 V vs. Zn/Zn^{2+} at sequential current densities of 0.025, 0.5, 0.3, 0.2 mA cm^{-2} in a single charging process. It was then galvanostatically discharged at 0.05 mA cm^{-2} to 0.8 V vs. Zn/Zn^{2+}.

The battery exhibited stable cycling capability, maintaining a stable specific capacity of 186.7 mAh g^{-1} with approximately 100% capacity retention over 850 cycles (Figure 3a). Additionally, the voltage profiles tracked throughout the testing process were consistent (Figure 3b,d), corresponding well with the fluctuating current profiles (Figure 3c,e). Overall, these results preliminarily indicate the aqueous Zn–I battery's compatibility with fluctuating charge operations, suggesting its potential for future integration with natural energy sources that exhibit fluctuating power.

Self-Discharge Performance

Self-discharge is a crucial factor in the practical application of batteries.[19,20] Minimizing the self-discharge rate is essential for ensuring a consistent energy supply, particularly in scenarios where natural energy sources may be intermittently available. To assess the self-discharge performance of the aqueous Zn–I battery, we conducted a series of tests after initially activating and charging the battery at 0.05 mA cm^{-2}. The battery was then

Research Article
doi.org/10.1002/batt.202400578
Chemistry Europe
European Chemical Societies Publishing

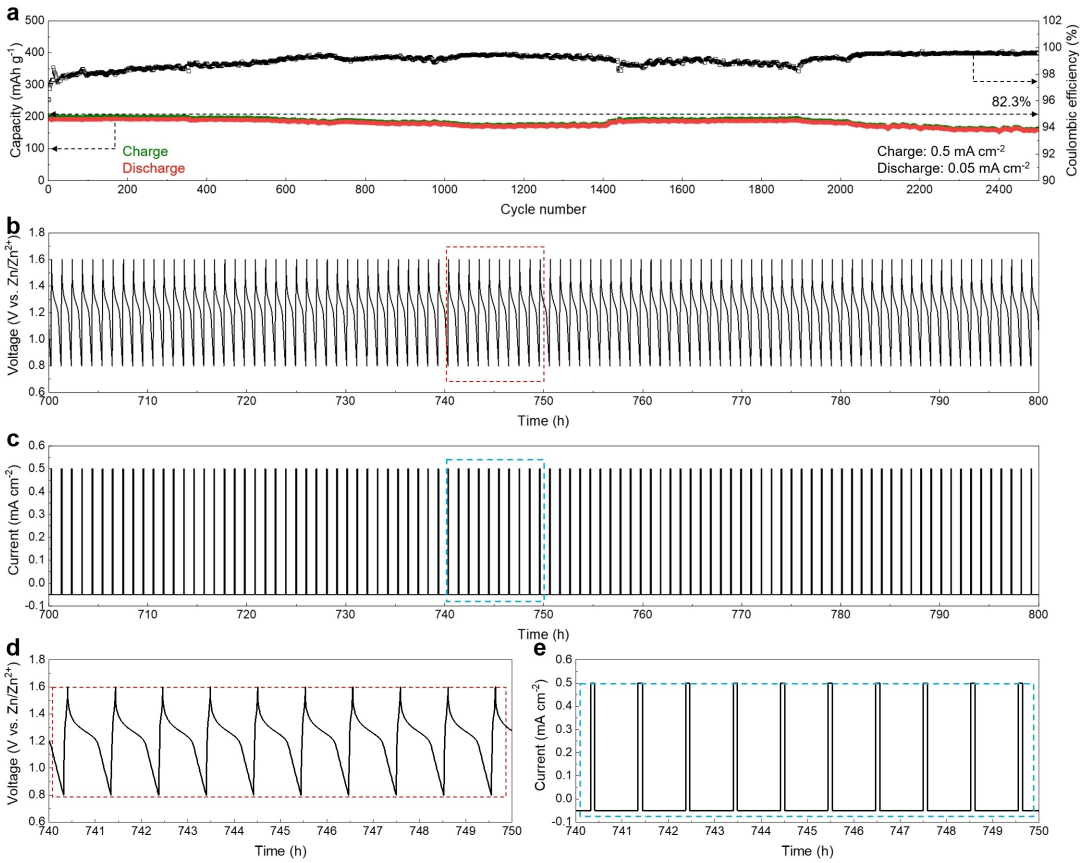

Figure 6. Fast-charging performance of the aqueous Zn–I battery. (a) Specific capacities and Coulombic efficiencies of the battery during tests. (b,d) Voltage and (c,e) current profiles of the battery during tests.

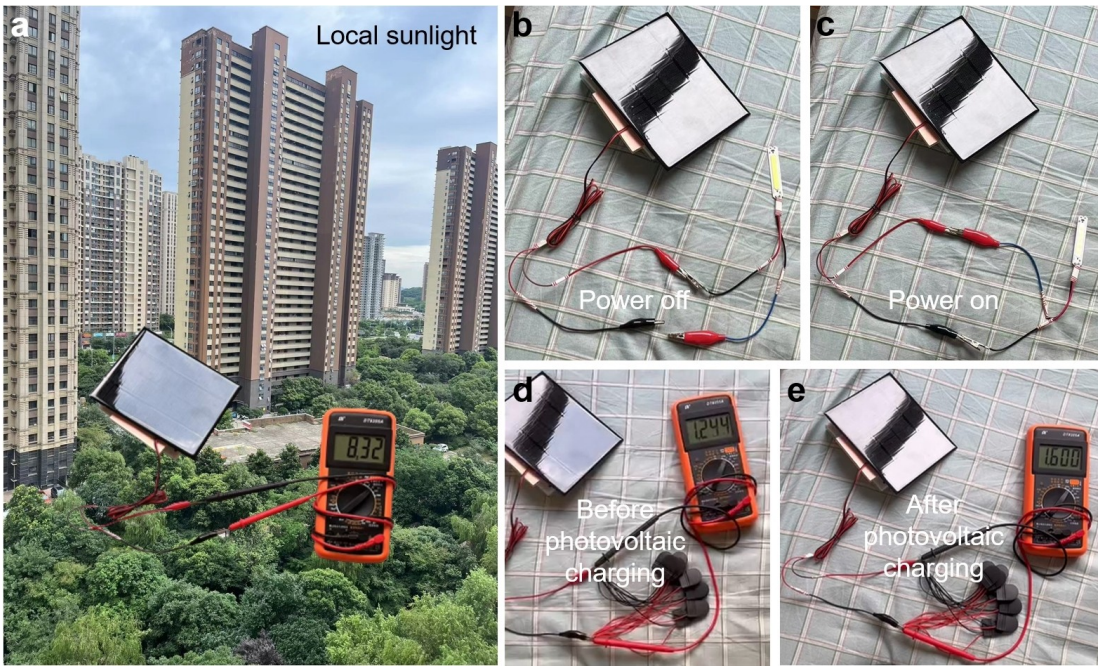

Figure 7. Practical integration potential of the aqueous Zn–I battery with photovoltaic solar panel charging. (a) Local sunlight during photovoltaic charging tests. (b,c) Photovoltaic solar panel not powering (b) and powering (c) a DC 12 V 1.5 W LED panel. (d,e) Battery voltage change before (d) and after (e) the photovoltaic solar panel charging the battery.

Research Article
doi.org/10.1002/batt.202400578
Chemistry Europe
European Chemical Societies Publishing

allowed to rest for 10, 50, 100, and 200 hours, respectively (Figure 4a). Following each resting period, the battery was discharged to 0.8 V vs. Zn/Zn^{2+} at 0.05 mA cm^{-2}. The battery showed a voltage drop of approximately 0.012 V during charging at 0.05 mA cm^{-2} (Figure S4, Supporting Information), indicating favorable electrochemical kinetics. The Coulombic efficiency, used to evaluate the self-discharge performance, revealed that the battery exhibited efficiencies of 73.5%, 56.3%, 49.9%, and 43.4% after resting for 10, 50, 100, and 200 hours, respectively (Figure 4b–e). These results indicate a decent decrease in capacity retention over extended rest periods, highlighting the need for further improvements to enhance the long-term self-discharge characteristics of the battery. Overall, this self-discharge test suggests that while the aqueous Zn–I battery shows promise, additional efforts are required to improve its capacity retention for prolonged use.

Compatibility with Various Charge Conditions

In practical applications, batteries often operate under partial charging conditions, such as in cell phones, electric vehicles, and other power supplies.[21,22] Ensuring compatibility with these conditions is crucial for practical use. To evaluate this, we tested the battery by charging it to various cutoff voltages of 1.6, 1.5, 1.4, 1.3, and 1.2 V vs. Zn/Zn^{2+} and discharging it to 0.8 V vs. Zn/Zn^{2+} repeatedly. The cycling test results showed that the battery exhibited stable cycling performance across these different charging voltages, indicating good compatibility with these various charging statuses (Figure 5a,b). Additionally, the battery maintained consistent charging voltage profiles at different charging cutoff voltages (Figure 5c). Furthermore, the battery demonstrated stable long-term cycling stability, retaining 85.1% of its specific capacity over 2000 cycles after testing its compatibility with various charging statuses (Figure 5d), and showed consistent voltage profiles (Figure 5e), indicating the battery cycling stability. These results indicate that the battery has a good compatibility with partial charging conditions and shows significant potential for practical applications.

Fast-Charging Performance

Fast-charging performance is a crucial factor in the development of modern batteries for both static and dynamic energy storage applications.[23,24] Although our battery is primarily designed for large-scale and static energy storage applications, it is essential to demonstrate decent fast-charging capabilities. To assess this, we conducted tests by glvanostatically charging the battery at 0.5 mA cm^{-2} and discharging it at 0.05 mA cm^{-2} repeatedly. The results showed that the battery maintained stable cycling performance with an 82.3% discharge capacity retention over 2500 cycles (Figure 6a). Throughout this test, the battery displayed consistent voltage profiles (Figure 6b,d) corresponding to the current profiles (Figure 6c,e). These results preliminarily indicates that the battery possesses good fast-charging capability, thereby enhancing its potential for practical applications.

Integration with Sustainable Power Supply

The ability to integrate batteries with practical power supplies is crucial for their adoption in real-world applications.[25,26] The integration capability of the aqueous Zn–I battery with a practical photovoltaic solar panel was demonstrated by charging the batteries using a 10 V-3 W-300 mA photovoltaic solar panel. Specifically, ten batteries connected in parallel were directly charged by the photovoltaic solar panel under local sunlight, resulting in an output voltage of 8.32 V (Figure 7a). Prior to the photovoltaic charging tests, the solar panel was evaluated by powering a DC-12 V-1.5 W LED panel. The photovoltaic solar panel successfully powered the LED lamps under local sunlight (Figure 7b,c). A multimeter was used to monitor voltage change of the batteries during the charging process with the photovoltaic solar panel. The batteries were successfully charged with the voltage increasing from 1.2 to 1.6 V vs. Zn/Zn^{2+} (Figure 7d,e and Video S7, Supporting Information). Subsequently, the DC-12 V-1.5 W LED panel was powered using the photovoltaic-charged aqueous Zn–I batteries connected in series, demonstrating successful energy output (Videos S8 and S9, Supporting Information). These demonstrations validate that the aqueous Zn–I battery exhibits good compatibility with practical photovoltaic charging, indicating its great potential for practical static energy storage applications.

Conclusions

In summary, we present an aqueous Zn–I battery utilizing the complexing effect between Zn^{2+} ions from the aqueous electrolyte and the amino functional group of PEI polymer in cathode. This complexing effect restricts the dissolution of inherently water-soluble PEI in the aqueous electrolyte, leading to the formation of insoluble PEI-Zn^{2+} complex. The PEI-Zn^{2+} complex serves as a fixation material to encapsulate the redox-active iodide species. The designed aqueous Zn–I battery demonstrated long-term cycling stability over 5000 cycles with an 83.3% capacity retention. Additionally, the battery showed compatibility with various operating conditions, including fluctuating charge currents, decent self-discharge rates, multiple charging statuses, and fast-charging capabilities. In conclusion, this cost-efficient and reliable battery construction concept leveraging the PEI-Zn^{2+} complexing effect provides au useful solution for advancing next-generation aqueous batteries with extended lifespans.

Acknowledgements

The authors are grateful to the support by the National Natural Science Foundation of China (22109069), the Natural Science Foundation of Jiangsu Province (BK20221446).

Conflict of Interests

The authors declare no conflict of interest.

Data Availability Statement

The data that support the findings of this study are available from the corresponding author upon reasonable request.

Keywords: Aqueous rechargeable Zn–I battery · PEI-Zn^{2+} complex · Long-lasting battery lifespan · Multiple operating conditions

[1] D. Lin, Y. Li, *Adv. Mater.* **2022**, *34*, 2108856.
[2] L. Tang, H. Peng, J. Kang, H. Chen, M. Zhang, Y. Liu, D. H. Kim, Y. Liu, Z. Lin, *Chem. Soc. Rev.* **2024**, *53*, 4877–4925.
[3] Y. Li, Z. Wang, Y. Cai, M. E. Pam, Y. Yang, D. Zhang, Y. Wang, S. Huang, *Energy Environ. Mater.* **2022**, *5*, 823–851.
[4] H. Chen, X. Li, K. Fang, H. Wang, J. Ning, Y. Hu, *Adv. Energy Mater.* **2023**, *13*, 2302187.
[5] Z. Zhu, T. Jiang, M. Ali, Y. Meng, Y. Jin, Y. Cui, W. Chen, *Chem. Rev.* **2022**, *122*, 16610–16751.
[6] Y. Feng, L. Zhou, H. Ma, Z. Wu, Q. Zhao, H. Li, K. Zhang, J. Chen, *Energy Environ. Sci.* **2022**, *15*, 1711–1759.
[7] Z. Bai, G. Wang, H. Liu, Y. Lou, N. Wang, H. K. Liu, S. Dou, *Chem. Sci.* **2024**, *15*, 3071–3092.
[8] H. Xu, W. Yang, M. Li, H. Liu, S. Gong, F. Zhao, C. Li, J. Qi, H. Wang, W. Peng, J. Liu, *Small* **2024**, *20*, 2310972.
[9] L. Zhang, H. Guo, W. Zong, Y. Huang, J. Huang, G. He, T. Liu, J. Hofkens, F. Lai, *Energy Environ. Sci.* **2023**, *16*, 4872–4925.
[10] H. Yu, Z. Wang, R. Zheng, L. Yan, L. Zhang, J. Shu, *Angew. Chem. Int. Ed.* **2023**, *135*, e202308397.
[11] P. Lin, G. Chen, Y. Kang, M. Zhang, J. Yang, Z. Lv, Y. Yang, J. Zhao, *ACS Nano* **2023**, *17*, 15492–15503.
[12] H. Liu, Z. Xu, B. Cao, Z. Xin, H. Lai, S. Gao, B. Xu, J.-L. Yang, T. Xiao, B. Zhang, H. J. Fan, *Adv. Energy Mater.* **2024**, *14*, 2400318.
[13] H. Fang, L. Lin, J. Chen, J. Wu, H. Tian, X. Chen, *Biomater. Sci.* **2019**, *7*, 1716–1728.
[14] C. Bertagnolli, A. Grishin, T. Vincent, E. Guibal, *Ind. Eng. Chem. Res.* **2016**, *55*, 2461–2470.
[15] T. Takagishi, S. Okuda, N. Kuroki, H. Kozuka, *J. Polym. Sci. Polym. Chem. Ed.* **1985**, *23*, 2109–2116.
[16] Y. Wei, K. A. M. Salih, M. F. Hamza, T. Fujita, E. Rodríguez-Castellón, E. Guibal, *Polymer* **2021**, *13*, 1513.
[17] U. Datta, A. Kalam, J. Shi, *Energy Storage* **2021**, *3*, e224.
[18] W. Wang, B. Yuan, Q. Sun, R. Wennersten, *J. Energy Storage* **2022**, *52*, 104812.
[19] H. O. Ford, E. S. Doyle, P. He, W. C. Boggess, A. G. Oliver, T. Wu, G. E. Sterbinsky, J. L. Schaefer, *Energy Environ. Sci.* **2021**, *14*, 890–899.
[20] Z. Huang, A. Chen, F. Mo, G. Liang, X. Li, Q. Yang, Y. Guo, Z. Chen, Q. Li, B. Dong, C. Zhi, *Adv. Energy Mater.* **2020**, *10*, 2001024.
[21] M. A. Hannan, M. S. H. Lipu, A. Hussain, A. Mohamed, *Renewable Sustainable Energy Rev.* **2017**, *78*, 834–854.
[22] C. Zhang, Y.-L. Wei, P.-F. Cao, M.-C. Lin, *Renewable Sustainable Energy Rev.* **2018**, *82*, 3091–3106.
[23] N. Wassiliadis, J. Schneider, A. Frank, L. Wildfeuer, X. Lin, A. Jossen, M. Lienkamp, *J. Energy Storage* **2021**, *44*, 103306.
[24] A. K. Thakur, M. S. Ahmed, H. Kang, R. Prabakaran, Z. Said, S. Rahman, R. Sathyamurthy, J. Kim, J.-Y. Hwang, *Adv. Energy Mater.* **2023**, *13*, 2202944.
[25] I. S. F. Gomes, Y. Perez, E. Suomalainen, *Renewable Sustainable Energy Rev.* **2020**, *126*, 109835.
[26] X. Luo, J. Wang, M. Dooner, J. Clarke, *Appl. Energy* **2015**, *137*, 511–536.

Manuscript received: September 30, 2024
Revised manuscript received: November 5, 2024
Accepted manuscript online: November 22, 2024
Version of record online: December 13, 2024